Computational evaluation of the chemical warfare agents capture performances of robust MOFs

C. Vieira Soares, A.A. Leitão, Guillaume Maurin

Computational Evaluation of the Chemical Warfare Agents Capture Performances of Robust MOFs

C. Vieira Soares, [a,b] A. A. Leitão [b] and G. Maurin [*a]

[a.] Institut Charles Gerhardt Montpellier, UMR-5253, Université de Montpellier, ENSCM, Place E. Bataillon, Montpellier cedex 05, 34095 (France).

[b.] Departamento de Química, Universidade Federal de Juiz de Fora, Juiz de Fora, MG, 36036-330, Brazil

Abstract

A series of stable MOFs containing zirconium or titanium ions as metal centers was screened to assess their capture performances for nerve agents including sarin and soman as well as their standard simulants, i.e. the dimethyl-methyl-phosphonate and diisopropyl fluorophosphate. These Monte Carlo simulations revealed that some of these MOFs show very high uptakes that significantly outperform those of other families of porous materials and interestingly they exhibit a very high affinity for these toxic molecules at low loading. These combined features make them potentially attractive to act as nerve agent filters. This set of adsorption data was further rationalized to establish structure-adsorption performances relationship and Monte Carlo simulations were combined with Density Functional Theory calculations to gain more insight into the adsorption mechanism in play. Finally, the choice of reliable simulants to accurately mimic the adsorption behavior of real toxic molecules in MOFs has been further discussed and in particular it has been established that soman is better

described considering the Pinacolyl methylphosphonate rather than the standard dimethyl-methyl-phosphonate and diisopropyl fluorophosphate simulants.

Keywords: MOFs, Chemical Warfare Agents, Monte Carlo simulations, Density Functional Theory calculations.

1. Introduction

Despite the chemical weapon convention of 1997, chemical warfare agents (CWAs) are still being employed throughout the world by terrorist groups and unscrupulous governments with most recently the reported use of CWAs in the Middle East [1]. This emphasizes that threat of exposure to CWAs is still considered as a major military issue. Several events such as the attack with sarin, in the Tokyo metro in 1995 [2], have also demonstrated that civilian populations may also be exposed to these toxic agents. Today's protection devices for the capture of CWA from air streams including gas masks and filters involve carbon materials (the so-called ASZM-TEDA [3]) impregnated with a mixture of nanoparticles of metal or metal oxides, salts and amines that act as specific adsorption sites for the targeted highly toxic molecules [4,5]. More recent developments have been also devoted to the detection of CWAs using notably pure or functionalized silica, zeolites, alumina or titania [6–8]. Although these existing adsorbents exhibit many desirable characteristics for the capture and the destruction of CWAs, they show relatively low adsorption capacities, rapid deactivation of their active sites and/or lack of tailorability. This leaves significant room to identify other porous materials with improved performances for such application. In this context, Metal-Organic Frameworks (MOFs) [9–13] have been recently envisaged as promising candidates for the identification, adsorption and/or catalytic degradation of CWAs [14]. The attractiveness of this family of hybrid porous ordered solids, built up from inorganic sub-units and organic complexing linkers bearing or not functional polar or apolar groups, lies in the huge spectrum of physical properties and chemistries that can be explored, where almost all of the elements of the periodic table have been used in one material or another. This offers an unprecedented opportunity to identify porous

adsorbents for CWA capture with the ability to capture a broad range of hazardous molecules to respond to diverse menaces and store high CWA. The large majority of studies related to the MOF/CWA topic has focused so far on the catalytic degradation purpose. The selected MOFs including Cu-BTC [15], MOF-5 [16], UiO-66s [17–19] UiO-67s [17,20], NU-1000 [17,21], PCN-222 [22], NENU-11 [23], Zn-DMCP [24], MIL-101(Al)-NH_2 [25] and MIL-53(Al)-NH_2 [25] revealed promising performances for the degradation of both G-type nerve agents, i.e. sarin, soman, VX and their standard simulants dimethyl-methyl-phosphonate (DMMP) and diisopropyl fluorophosphate (DIFP), and vesicant agents of which sulphur mustard and its simulant including 2-chloroethylethylsulfide (CEES). In terms of adsorption studies, only a very few studies have been reported. We can cite the experimental studies on the adsorption of DMMP in NENU-11 and MOF-5 [16] while a first computational exploration has been very recently published by Matito-Martos *et al.* on the CWA removal capacity performances of a large series of MOFs [26]. Some of the tested MOFs for CWA-related applications are unstable in the presence of water which hampers their use for CWA capture since humidity in the air and in the breath is usually present in operating conditions.

In this context, priority has to be given to explore the CWA capture in chemical stable MOF containing high-valent cations, e.g. Al^{3+}, Zr^{4+}, Ti^{4+}, as metal centers to ensure that the performances can be maintained under operating conditions over prolonged periods. Another requirement is to favor MOFs incorporating relatively cheap commercially available organic linkers, easily scaled-up, and prepared via green synthesis routes in order to be cost-competitive with respect to the ASZM-TEDA active carbons currently used as filters. With these ideas in mind, here we report a systematic computational evaluation of the CWA capture performances of a series of Zr- and Ti- MOFs, showing

different pore size/topology and incorporating diverse adsorption sites (Fig. 1), that have been proved to be water stable. This study aimed to explore sarin and soman as well as their most common simulants used in experiments, i.e. DMMP, DIFP and Pinacolyl methylphosphonate (PMP) (Fig. 2). Grand Canonical Monte Carlo (GCMC) simulations have been combined with Density Functional Theory (DFT) calculations to assess the adsorption uptakes and the energetics for each MOF/CWA pair and to evidence the preferential adsorption sites and the resulting CWA/MOF interactions. As a further step, this computational database has been used to build model structure-adsorption performances in order to identify the key parameters of the MOFs that drive the CWA capture. Finally, the comparison of the simulated adsorption behaviors of CWA and their simulants allowed us to define the most reliable simulant that mimics as fairly as possible the real molecules.

2. Computational details

The structural models for all MOFs were taken from the literature: MIL-125-(Ti) and MIL-125-(Ti)-NH_2 [27]; MIL-140-D [28], MIL-140-E and MIL-140G [29]; MIP-177 and MIP-177-OH-H_2O [30]; MIP-200 and MIP-200-OH-H_2O [31]; MOF-808-A, MOF-808-F, MOF-808-P and MOF-808-OH-H_2O [32]; NU-1000 [33]; UiO-66-(Zr) [34]; UiO-66-(Zr)-Cl, UiO-66-(Zr)-$(OH)_2$, UiO-66-(Zr)-CO_2H, UiO-66-(Zr)-NO_2 and UiO-66-(Zr)-NH_2 [35]; defective UiO-66-(Zr) and UiO-66-(Zr)-NH_2 labelled as UiO-66-(Zr)-defects3 and UiO-66-(Zr)-NH_2 defects6 respectively in a previous study [36]; UiO-67-(Zr) [34], UiO-68-(Zr) [34] and Zr_6-AZO-BDC [37] (Figures S1-S25). The structures of MIP-177-OH-H_2O, MIP-200-OH-H_2O, MOF-808-OH-H_2O and defective UiO-66-(Zr) and UiO-66-(Zr)-NH_2 were preliminary saturated by hydroxyl and water groups. These atoms were added to the metal atoms of the inorganic nodes. All crystal structures were

further geometry optimized at the DFT level keeping the experimental unit cell parameters fixed. These calculations were performed using the Perdew Burke Ernzerhof (PBE) functional at generalized gradient approximation (GGA) [38] combined with the Double Numeric basis set with Polarization functions (DNP) [39] on all atoms as implemented in DMol^3 package [40].

2.1 *Force fields*

The interactions between MOFs and CWAs were treated using the sum of a 12-6 Lennard-Jones (LJ) contribution and a Coulombic term. The Universal force field (UFF) [41] and DREIDING [42] force field were adopted to describe the Lennard-Jones (LJ) parameters of all atoms of the inorganic nodes and the organic linkers, respectively. The partial charges for all atoms of the MOF frameworks were extracted from our DFT calculations (see Tables S1-S25 and corresponding Figures S1-S25). Regarding the CWAs, sarin, soman and DMMP molecules were described by a united atom representation including LJ point charges with parameters taken from the transferable potentials for phase equilibria (TraPPE) force field, reported by Sokkalingam et al. [43]. Same united atom representations were considered for the DIFP and PMP molecules with parameters taken from the previous work reported by Vishnyakov et al. [44] and Sokkalingam et al. [43] respectively. The LJ cross parameters corresponding to the interactions between the CWAs and the MOFs framework were obtained using the Lorentz-Berthelot mixing rules. Finally, the charges of these CWAs were taken from these previously reported United Atom models of these molecules as illustrated in Figure 2.

2.2 *Monte Carlo simulations*

Grand Canonical Monte Carlo (GCMC) simulations were performed at 298 K for all MOFs and CWAs selected in this work for a series of fugacity for the CWAs up to 5000 kPa in order to estimate the saturation capacity for each molecule. The selection of this high range of pressure is to make sure that we can assess the maximum payload of all MOFs and there is no link with the pressure encountered under working condition of nerve agent filters. These calculations were performed using the Complex Adsorption and Diffusion Simulation Suite (CADSS) code implementing the configurational-bias Monte Carlo scheme that was used in this study to favor a more efficient sampling of the CWAs in the pores of the MOFs. This method includes insertion/deletion, translational, rotational, partial and full regrowth MC steps. The simulation box considered for all MOFs was defined in such a way that all a, b and c dimensions were longer than 24 Å. Short-range dispersion forces described by LJ potentials were thus truncated at a cutoff radius of 12 Å, whereas long-range electrostatic interactions were handled using the Ewald summation technique. For each state point, 2×10^8 Monte Carlo steps have been used for both equilibration and production runs. The adsorption enthalpies at low coverage (ΔH) for each molecule were calculated for all MOFs using the revised Widom's test particle insertion method [45]. To gain insight into the arrangement of the CWAs in the pores of the MOFs, the CWA/CWA and CWA/MOF radial distribution functions (RDFs) were obtained by averaging over the whole configurations generated during the GCMC simulations.

2.3 *Density Functional Theory calculations*

A Bader charge analysis was conducted on the MOF/CWA systems using a grid-based algorithm [46] to analyse the potential charge transfer between the CWAs and the MOFs. The charge in all atoms of the system was defined as the difference between the valence charge and the Bader charge. These calculations were performed using the codes available in the Quantum-Espresso package [47], which implements the Density Functional Theory (DFT) [48,49] with periodic boundary conditions using plane wave functions as basis set [50]. We used the generalized gradient approximation (GGA/PBE) [51] for the exchange-correlation functional, and the ion cores of atoms were described by the Vanderbilt [52] ultrasoft pseudopotential. These calculations were performed using single point calculation on the configuration generated by the MC simulations.

3. Results and discussion

Figure 3 reports the simulated CWA uptakes for all MOFs. One can observe that the best materials for CWA capture are MOF-808s, NU-1000, UiO-68(Zr) and Zr-Azo-BDC. This conclusion remains valid for all real CWAs and their simulants with adsorption uptakes above 6 mmol/g. This level of performances significantly surpasses that of previously reported MOFs and other standard porous materials. Typically, the carbons adsorb much lower amounts of CWAs. As an illustration Kowalczyk et al. [53], demonstrated that pitch-based P7 Activated Carbon Fiber (ACF) and the commercialized Norit activated carbons adsorb only respectively 0.806 $mmol.g^{-1}$ and 0.161 $mmol.g^{-1}$ of DMMP. In addition, the current activated carbon ASZM-TEDA showed a sarin adsorption uptake of 0.04 mg/m^3 [54]. Regarding MOFs, as mentioned in the introduction only a very few studies have been reported on their CWA adsorption performances. We can cite the sodalite-type MOF (NENU-11) [23] and MOF-5 [16]

that were shown to adsorb 1.92 mmol.g^{-1} and 7.3 mmol.g^{-1} of DMMP respectively. As a further step, we concentrated our effort to identify the features of the MOFs at the origin of these high CWA uptakes. We evidenced that the uptake of each CWA considered individually correlates rather well with the N_2-accessible surface area calculated for the MOFs (see Table S26 and Figure S26 - correlation factors R^2 varying from 0.84 to 0.90). The correlation is even better using the free pore volume as a descriptor of the MOFs (see Figure S27 with correlation factors higher than 0.96). In order to obtain a more generic expression, we introduced another geometric descriptor labelled as α which is given by the following expression: $\alpha = \left(\frac{V_{MOF}}{\frac{v_{Soman}}{v_{CWA}}}\right)$, where V_{MOF} corresponds to the free pore volume of the MOF, v_{Soman} and v_{CWA} are the volume of the bulkier CWA, i.e. soman, and the other molecules respectively. Figure 4 evidences an excellent correlation between the uptakes and α for all MOFs (correlation factor R^2 of 0.99). This structure-adsorption uptake performance relationship emphasizes that the capacity of stockpiling CWA in MOFs is predominantly governed by a pore filling mechanism, the higher porosity leading to the higher CWA uptake. This structure-adsorption uptake performance relationship emphasizes that the capacity of stockpiling CWA in MOFs is predominantly governed by a pore filling mechanism, the higher porosity leading to the higher CWA uptake. The predominance of this mechanism is also supported by the excellent correlation for all CWAs between the uptake capacity of the MOF with the fraction of the free pore volume of the MOF and the volume of the adsorbed molecule $\left(\frac{V_{MOF}}{v_{CWA}}\right)$ as reported in Figure S28. Typically, the best materials UiO-68(Zr) and MOF-808s show the highest free pore volumes of 1.75 and 1.85 cm^3.g^{-1} respectively (see Table S26).

We further evidenced that the calculated adsorption enthalpy is higher for all CWAs in the case of the MOFs showing the lower free pore volume although we do not find a direct correlation since the chemical features of the MOFs also impact the CWA/MOF interactions (see Figure S29). This observation is consistent with the systematic computational study reported by Agrawal *et al*, which demonstrated that the MOFs with the pore limiting diameters in the range of 6-8 Å show the highest affinity for Sarin [55].

Interestingly the calculated CWA adsorption enthalpies were shown to be spread in a relatively large domain reaching for some MOFs very high values up to -110 kJ/mol. The strength of interactions obtained for these screened MOFs is significantly higher than the unique experimental value reported so far for a MOF, i.e. -44.8 kJ/mol for DIFP in Zn-DMCP [24].

To gain more insight into the microscopic origin of the potentially high CWA/MOF interactions, a carefully analysis of the preferential adsorption sites for the CWAs was undertaken based on the calculations of the radial distribution functions for the diverse CWA/MOF atom pairs averaged over the whole configurations generated by Monte Carlo simulations. Typically, we detailed the scenario for the defective UiO-66-(Zr)-NH_2 which is one of the MOFs showing the stronger interactions with sarin, soman, DMMP and DIFP associated with adsorption enthalpies of -108, -95, -93 and -94 kJ mol^{-1} respectively. It is not be noted that these values converge well with the interaction energies calculated at the DFT-level (Table S26). This observation validates the set of LJ potential parameters and atomic partial charges used to describe the CWA/MOF interactions. Figure 5a shows that sarin is preferentially located in the vicinity of the amino function grafted to the organic linker via an interaction between its oxygen atom

of the P=O group and the hydrogen atom of the amino group with a characteristic distance of 2.7 Å. Such a range of interacting distance suggests a relatively moderated strength of interaction between CWA and the MOFs and thus a physisorption-based process. The same preferential interactions with the NH_2-group of the MOF were also observed for the simulants DMMP and DIFP (Figures 5c and 5d) while the adsorption behavior of soman only slightly deviates with an interaction between its oxygen atom of the P=O group and the hydrogen atom of the hydroxyl group bounded to the Zr atom (Figure 5b). Relatively similar strength of CWA/MOFs interactions and microscopic adsorption mechanisms were also observed for the other best MOFs including for instance MOF-808s (Figure S30).

In order to confirm that the CWA adsorption proceeds in these MOFs via physisorption-type interactions, we performed further DFT analysis. As a typical example, we specifically treated the case of CWA adsorbed in the defective UiO-66(Zr)-NH_2. The analysis of Bader charges revealed that there is no significant change when one compares the charges of the isolated and confined CWA as summarized in Table 1. This result clearly supports that there is no charge transfer between the CWA and the host framework and this excludes the existence of a chemisorption process.

From an experimental standpoint, simulant molecules, with physical or chemical properties similar to the real CWAs are usually considered to avoid working with the highly toxic agents. DMMP and DIFP are the most common simulants employed to mimic soman and sarin respectively, however it is crucial to make sure that they accurately capture the adsorption behaviour of the real molecules and this issue has been only rarely discussed so far in the literature. In this concern, Agrawal et al. [55] showed that dimethyl p-nitrophenyl phosphate (DMNP) is a suitable simulant to mimic

the adsorption of Soman while DMMP, DIFP and diethyl chlorophosphite are more appropriate to reproduce the behavior of Sarin. To address this question in the case of MOFs, we considered the comparison of the adsorption behaviours of DIFP, DMMP, soman and sarin in two representative MOFs, namely the MOF-808-OH-H_2O and the MIP-177-OH-H_2O. Table 2 shows the simulated adsorption uptakes and adsorption enthalpies for all four molecules. It can be clearly stated that while DMMP and DIFP accurately reproduce the behavior of sarin in terms of uptake and energetics this is far to be the case for soman. Therefore, we searched for an alternative simulant that can mimic more accurately soman. Indeed, the PMP molecule showing similar backbone than the real molecule (see Figure 2) was thus considered. Table 2 indicates that this simulant reproduces much better the adsorption behavior of soman (in terms of both uptake and energetics), Figure S31 showing that it occupies a preferential sitting in the pores similar to the real molecule. This observation suggests that this simulant of low toxicity should be considered as an alternative to the standard DMMP and DIFP molecules to explore the performances of MOFs regarding soman.

4. Conclusions

In summary, our GCMC simulations evidenced that a series of water stable Zr and Ti MOFs show outstanding adsorption uptakes for soman, sarin and their simulants combined with high adsorption enthalpies. This level of performance makes these materials potentially attractive as CWA filters with great promises in large payload and limitation of release under operating conditions. Although the CWA adsorption enthalpies reached for some MOFs values higher than -100 $kJ.mol^{-1}$, complementary DFT analysis precluded the existence of charge transfer between the CWA and the host

framework consistent with a physisorption-based process involving mostly van der Waals interactions. Structure-CWA adsorption performances relationship was established with the definition of a geometric descriptor based on the free pore volume of the MOF and the molecular dimension of the CWAs. Finally, we evidenced that a special attention needs to be paid when one selects the simulants to mimic the adsorption of real CWAs in MOFs. While the standard DMMP and DIFP simulants reproduce well the behavior of sarin, this is not anymore true for soman and we established that an alternative simulant, namely the PMP molecule, needs to be considered. A further step will be to consider the competitive adsorption of CWAs with water and hydrocarbons to confirm the viability of these promising MOFs as CWA filters. Furthermore, such a computational approach can be applied in order to explore the adsorption performances of other materials with respect to different families of CWAs and toxic industrial compounds (TICs).

Conflicts of interest

There are no conflicts to declare.

Acknowledgements

The research leading to these results has received funding from a bilateral project COFECUB-CAPES 778-13. G.M. thanks the Institut Universitaire de France for its support.

References

[1] Chemical attack of 7 April 2018 (Douma, Eastern Ghouta, Syria) Syria's clandestine chemical weapons programme, 2018 (2018) 1–7.

[2] B.M. Smith, Catalytic methods for the destruction of chemical warfare agents under ambient

conditions., Chem. Soc. Rev. 37 (2008) 470–478. doi:10.1039/b705025a.

[3] J.B. Decoste, G.W. Peterson, Metal – Organic Frameworks for Air Puri fi cation of Toxic Chemicals, (2014).

[4] J. V. Romero, J.W.H. Smith, B.M. Sullivan, M.G. Mallay, L.M. Croll, J.A. Reynolds, C. Andress, M. Simon, J.R. Dahn, Gas adsorption properties of the ternary ZnO/CuO/CuCl 2 impregnated activated carbon system for multigas respirator applications assessed through combinatorial methods and dynamic adsorption studies, ACS Comb. Sci. 13 (2011) 639–645. doi:10.1021/co200121c.

[5] J.W.H. Smith, J. V. Romero, T.R. Dahn, K. Dunphy, L.M. Croll, J.R. Dahn, The effect of co-impregnated acids on the performance of Zn-based broad spectrum respirator carbons, J. Hazard. Mater. 235–236 (2012) 279–285. doi:10.1016/j.jhazmat.2012.07.061.

[6] A. Saxena, A.K. Srivastava, B. Singh, A. Goyal, Removal of sulphur mustard , sarin and simulants on impregnated silica nanoparticles, J. Hazard. Mater. 211–212 (2012) 226–232. doi:10.1016/j.jhazmat.2011.07.117.

[7] A.K. Verma, A.K. Srivastava, B. Singh, D. Shah, S. Shrivastava, C. Kant, P. Shinde, Chemosphere Alumina-supported oxime for the degradation of sarin and diethylchlorophosphate, Chemosphere. 90 (2013) 2254–2260. doi:10.1016/j.chemosphere.2012.10.011.

[8] D.A. Panayotov, J.R. Morris, Uptake of a Chemical Warfare Agent Simulant (DMMP) on TiO 2 : Reactive Adsorption and Active Site Poisoning, (2009) 3652–3658.

[9] G. Férey, Hybrid porous solids: past, present, future, Chem. Soc. Rev. 37 (2008) 191–214. doi:10.1039/B618320B.

[10] B.F. Hoskins, R. Robson, Infinite Polymeric Frameworks Consisting of Three Dimensionally Linked Rod-like Segments, J. Am. Chem. Soc. 111 (1989) 5962–5964. doi:10.1021/ja00197a079.

[11] O.M. Yaghi, H. Li, Hydrothermal Synthesis of a Metal-Organic Framework Containing Large Rectangular Channels, J. Am. Chem. Soc. 117 (1995) 10401–10402. doi:10.1021/ja00146a033.

[12] K. Mitsuru, Y. Tomomichi, M. Hiroyuki, K. Susumu, S. Kenji, Three-Dimensional Framework

with Channeling Cavities for Small Molecules: {[M2(4, 4′-bpy)3(NO3)4]·xH2O}n (M □ Co, Ni, Zn), Angew. Chemie Int. Ed. English. 36 (2003) 1725–1727. doi:doi:10.1002/anie.199717251.

[13] G. Maurin, C. Serre, A. Cooper, G. Férey, The new age of MOFs and of their porous-related solids, Chem. Soc. Rev. 46 (2017) 3104–3107. doi:10.1039/c7cs90049j.

[14] N.S. Bobbitt, M.L. Mendonca, A.J. Howarth, T. Islamoglu, J.T. Hupp, O.K. Farha, R.Q. Snurr, Metal–organic frameworks for the removal of toxic industrial chemicals and chemical warfare agents, Chem. Soc. Rev. 46 (2017) 3357–3385. doi:10.1039/C7CS00108H.

[15] A. Roy, A.K. Srivastava, B. Singh, D. Shah, T.H. Mahato, P.K. Gutch, A.K. Halve, Degradation of sarin, DEClP and DECNP over Cu-BTC metal organic framework, J. Porous Mater. 20 (2013) 1103–1109. doi:10.1007/s10934-013-9692-4.

[16] Z. Ni, J.P. Jerrell, K.R. Cadwallader, R.I. Masel, Metal-organic frameworks as adsorbents for trapping and preconcentration of organic phosohonates, Anal. Chem. 79 (2007) 1290–1293. doi:10.1021/ac0613075.

[17] T. Islamoglu, M.A. Ortuño, E. Proussaloglou, A.J. Howarth, N.A. Vermeulen, A. Atilgan, A.M. Asiri, C.J. Cramer, O.K. Farha, Presence versus Proximity: The Role of Pendant Amines in the Catalytic Hydrolysis of a Nerve Agent Simulant, Angew. Chemie - Int. Ed. 57 (2018) 1949–1953. doi:10.1002/anie.201712645.

[18] M.J. Katz, S.-Y. Moon, J.E. Mondloch, M.H. Beyzavi, C.J. Stephenson, J.T. Hupp, O.K. Farha, Exploiting parameter space in MOFs: a 20-fold enhancement of phosphate-ester hydrolysis with UiO-66-NH2, Chem. Sci. 6 (2015) 2286–2291. doi:10.1039/C4SC03613A.

[19] M.R. Momeni, C.J. Cramer, Dual Role of Water in Heterogeneous Catalytic Hydrolysis of Sarin by Zirconium-Based Metal–Organic Frameworks, ACS Appl. Mater. Interfaces. 10 (2018) 18435–18439. doi:10.1021/acsami.8b03544.

[20] S.Y. Moon, G.W. Wagner, J.E. Mondloch, G.W. Peterson, J.B. DeCoste, J.T. Hupp, O.K. Farha, Effective, Facile, and Selective Hydrolysis of the Chemical Warfare Agent VX Using Zr6-Based Metal-Organic Frameworks, Inorg. Chem. 54 (2015) 10829–10833.

doi:10.1021/acs.inorgchem.5b01813.

[21] J.E. Mondloch, M.J. Katz, W.C. Isley III, P. Ghosh, P. Liao, W. Bury, G.W. Wagner, M.G. Hall, J.B. DeCoste, G.W. Peterson, R.Q. Snurr, C.J. Cramer, J.T. Hupp, O.K. Farha, Destruction of chemical warfare agents using metal–organic frameworks, Nat. Mater. 14 (2015) 512–516. doi:10.1038/nmat4238.

[22] P. Li, R.C. Klet, S.-Y. Moon, T.C. Wang, P. Deria, A.W. Peters, B.M. Klahr, H.-J. Park, S.S. Al-Juaid, J.T. Hupp, O.K. Farha, Synthesis of nanocrystals of Zr-based metal–organic frameworks with csq-net: significant enhancement in the degradation of a nerve agent simulant, Chem. Commun. 51 (2015) 10925–10928. doi:10.1039/C5CC03398E.

[23] F.J. Ma, S.X. Liu, C.Y. Sun, D.D. Liang, G.J. Ren, F. Wei, Y.G. Chen, Z.M. Su, A sodalite-type porous metal-organic framework with polyoxometalate templates: Adsorption and decomposition of dimethyl methylphosphonate, J. Am. Chem. Soc. 133 (2011) 4178–4181. doi:10.1021/ja109659k.

[24] C. Montoro, F. Linares, E. Quartapelle Procopio, I. Senkovska, S. Kaskel, S. Galli, N. Masciocchi, E. Barea, J.A.R. Navarro, Capture of nerve agents and mustard gas analogues by hydrophobic robust MOF-5 type metal-organic frameworks, J. Am. Chem. Soc. 133 (2011) 11888–11891. doi:10.1021/ja2042113.

[25] L. Bromberg, Y. Klichko, E.P. Chang, S. Speakman, C.M. Straut, E. Wilusz, T.A. Hatton, Alkylaminopyridine-modified aluminum aminoterephthalate metal-organic frameworks as components of reactive self-detoxifying materials, ACS Appl. Mater. Interfaces. 4 (2012) 4595–4602. doi:10.1021/am3009696.

[26] I. Matito-Martos, P.Z. Moghadam, A. Li, V. Colombo, J.A.R. Navarro, S. Calero, D. Fairen-Jimenez, Discovery of an Optimal Porous Crystalline Material for the Capture of Chemical Warfare Agents, Chem. Mater. 30 (2018) 4571–4579. doi:10.1021/acs.chemmater.8b00843.

[27] M. Dan-hardi, C. Serre, L. Rozes, G. Maurin, A New Photoactive Crystalline Highly Porous Titanium (IV) Dicarboxylate, J. Am. Chem. Soc. 131 (2009) 1–15. doi:10.1021/ja903726m.

[28] V. Guillerm, F. Ragon, M. Dan-Hardi, T. Devic, M. Vishnuvarthan, B. Campo, A. Vimont, G. Clet, Q. Yang, G. Maurin, G. Férey, A. Vittadini, S. Gross, C. Serre, A series of isoreticular, highly stable, porous zirconium oxide based metal-organic frameworks, Angew. Chemie - Int. Ed. 51 (2012) 9267–9271. doi:10.1002/anie.201204806.

[29] C. Serre, A private communication, (2018).

[30] S. Wang, T. Kitao, N. Guillou, M. Wahiduzzaman, C. Martineau-Corcos, F. Nouar, A. Tissot, L. Binet, N. Ramsahye, S. Devautour-Vinot, S. Kitagawa, S. Seki, Y. Tsutsui, V. Briois, N. Steunou, G. Maurin, T. Uemura, C. Serre, A phase transformable ultrastable titanium-carboxylate framework for photoconduction, Nat. Commun. 9 (2018) 1660. doi:10.1038/s41467-018-04034-w.

[31] and C.S. Sujing Wang, Ji Sun Lee, Mohammad Wahiduzzaman, Jaedeuk Park, Mégane Muschi1, Charlotte Martineau-Corcos, Antoine Tissot, Kyung Ho Cho, Jérôme Marrot, William Shepard, Guillaume Maurin, Jong-San Chang, A Robust Energy-Efficient Metal-Organic Framework Adsorbent for Refrigeration, Nat. Energy. (n.d.) under revision.

[32] W. Liang, H. Chevreau, F. Ragon, P.D. Southon, V.K. Peterson, D.M. D'Alessandro, Electronic Supporting Information Tuning pore size in a zirconium-tricarboxylate metal-organic framework, CrystEngComm. 16 (2014) 6530–6533. doi:10.1039/c4ce01031k.

[33] J.E. Mondloch, W. Bury, D. Fairen-Jimenez, S. Kwon, E.J. Demarco, M.H. Weston, A.A. Sarjeant, S.T. Nguyen, P.C. Stair, R.Q. Snurr, O.K. Farha, J.T. Hupp, Vapor-phase metalation by atomic layer deposition in a metal-organic framework, J. Am. Chem. Soc. 135 (2013) 10294–10297. doi:10.1021/ja4050828.

[34] J.H.H. Cavka, S. Jakobsen, U. Olsbye, N. Guillou, C. Lamberti, S. Bordiga, K.P.P. Lillerud, A New Zirconium Inorganic Building Brick Forming Metal Organic Frameworks with Exceptional Stability, 130 (2008) 13850–13851. doi:10.1021/ja8057953.

[35] Q. Yang, A.D. Wiersum, P.L. Llewellyn, V. Guillerm, C. Serre, G. Maurin, Functionalizing porous zirconium terephthalate UiO-66(Zr) for natural gas upgrading: a computational exploration, Chem. Commun. 47 (2011) 9603. doi:10.1039/c1cc13543k.

[36] S.M.J. Rogge, J. Wieme, L. Vanduyfhuys, S. Vandenbrande, G. Maurin, T. Verstraelen, M. Waroquier, V. Van Speybroeck, Thermodynamic Insight in the High-Pressure Behavior of UiO-66: Effect of Linker Defects and Linker Expansion, Chem. Mater. 28 (2016) 5721–5732. doi:10.1021/acs.chemmater.6b01956.

[37] A. Schaate, S. Dühnen, G. Platz, S. Lilienthal, A.M. Schneider, P. Behrens, A novel Zr-based porous coordination polymer containing azobenzenedicarboxylate as a linker, Eur. J. Inorg. Chem. (2012) 790–796. doi:10.1002/ejic.201101151.

[38] J.P. Perdew, K. Burke, M. Ernzerhof, Generalized gradient approximation made simple, Phys. Rev. Lett. 77 (1996) 3865–3868. doi:10.1103/PhysRevLett.77.3865.

[39] W.J. Hehre, K. Ditchfield, J.A. Pople, Self-consistent molecular orbital methods. XII. Further extensions of gaussian-type basis sets for use in molecular orbital studies of organic molecules, J. Chem. Phys. 56 (1972) 2257–2261. doi:10.1063/1.1677527.

[40] B. Delley, From molecules to solids with the DMol3 approach, J. Chem. Phys. 113 (2000) 7756–7764. doi:10.1063/1.1316015.

[41] A.K. Rappé, C.J. Casewit, K.S. Colwell, W.A. Goddard, W.M. Skiff, UFF, a Full Periodic Table Force Field for Molecular Mechanics and Molecular Dynamics Simulations, J. Am. Chem. Soc. 114 (1992) 10024–10035. doi:10.1021/ja00051a040.

[42] S.L. Mayo, B.D. Olafson, W.A. Goddard, DREIDING: A generic force field for molecular simulations, J. Phys. Chem. 94 (1990) 8897–8909. doi:10.1021/j100389a010.

[43] N. Sokkalingam, G. Kamath, M. Coscione, J.J. Potoff, Extension of the transferable potentials for phase equilibria force field to dimethylmethyl phosphonate, sarin, and soman, J. Phys. Chem. B. 113 (2009) 10292–10297. doi:10.1021/jp903110e.

[44] A. Vishnyakov, G.Y. Gor, M.T. Lee, A. V. Neimark, Molecular modeling of organophosphorous agents and their aqueous solutions, J. Phys. Chem. A. 115 (2011) 5201–5209. doi:10.1021/jp200509u.

[45] T.J.H. Vlugt, E. García-Pérez, D. Dubbeldam, S. Ban, S. Calero, Computing the Heat of

Adsorption using Molecular Simulations: The Effect of Strong Coulombic Interactions, J. Chem. Theory Comput. 4 (2008) 1107–1118. doi:10.1021/ct700342k.

[46] G. Henkelman, A. Arnaldsson, H. Jónsson, A fast and robust algorithm for Bader decomposition of charge density, Comput. Mater. Sci. 36 (2006) 354–360. doi:10.1016/j.commatsci.2005.04.010.

[47] P. Giannozzi, S. Baroni, N. Bonini, M. Calandra, R. Car, C. Cavazzoni, D. Ceresoli, G.L. Chiarotti, M. Cococcioni, I. Dabo, A. Dal Corso, S. De Gironcoli, S. Fabris, G. Fratesi, R. Gebauer, U. Gerstmann, C. Gougoussis, A. Kokalj, M. Lazzeri, L. Martin-Samos, N. Marzari, F. Mauri, R. Mazzarello, S. Paolini, A. Pasquarello, L. Paulatto, C. Sbraccia, S. Scandolo, G. Sclauzero, A.P. Seitsonen, A. Smogunov, P. Umari, R.M. Wentzcovitch, QUANTUM ESPRESSO: A modular and open-source software project for quantum simulations of materials, J. Phys. Condens. Matter. 21 (2009). doi:10.1088/0953-8984/21/39/395502.

[48] P.& K. Hohenberg, Inhomogeneous electron gas, Phys. Rev. B. 136 (1964) B864–B871. doi:10.1103/PhysRevB.7.1912.

[49] W. Kohn, L.J. Sham, Self-consistent equations including exchange and correlation effects, Phys. Rev. 140 (1965). doi:10.1103/PhysRev.140.A1133.

[50] G. Makov, M.C. Payne, Periodic boundary conditions in ab initio calculations, Phys. Rev. B. 51 (1995) 4014–4022. doi:10.1103/PhysRevB.51.4014.

[51] J.P. Perdew, Y. Wang, Accurate and simple analytic representation of the electron-gas correlation energy, Phys. Rev. B. 45 (1992) 13244–13249. doi:10.1103/PhysRevB.45.13244.

[52] D. Vanderbilt, Soft self-consistent pseudopotentials in a generalized eigenvalue formalism, Phys. Rev. B. 41 (1990) 7892–7895. doi:10.1103/PhysRevB.41.7892.

[53] P. Kowalczyk, P.A. Gauden, A.P. Terzyk, A. V. Neimark, Screening of carbonaceous nanoporous materials for capture of nerve agents, Phys. Chem. Chem. Phys. 15 (2013) 291–298. doi:10.1039/C2CP43366D.

[54] Office of Research and Development National Homeland Security Research, Adsorption and

Desorption of Chemical Warfare Agents on Activated Carbon : Impact of Temperature and Relative Humidity Adsorption and Desorption of Chemical Warfare Agents on Activated Carbon : Impact of Temperature and Relative Humidity, 2014.

[55] M. Agrawal, D.F. Sava Gallis, J.A. Greathouse, D.S. Sholl, How Useful Are Common Simulants of Chemical Warfare Agents at Predicting Adsorption Behavior?, J. Phys. Chem. C. 122 (2018) 26061–26069. doi:10.1021/acs.jpcc.8b08856.

Table 1

Bader charge analysis for the isolated and adsorbed CWAs in the defective UiO-66(Zr)-NH_2.

Charges	Isolated Soman	Confined Soman	Isolated Sarin	Confined Sarin	Isolated DMMP	Confined DMMP	Isolated DIFP	Confined DIFP
O=(P)	-1.87	-1.88	-1.88	-1.88	-1.88	-1.87	-1.88	-1.88
O-CH	-1.71	-1.71	-1.71	-1.71	-	-1.70	-1.71	-1.70
P	4.86	4.86	4.86	4.86	4.86	4.86	4.86	4.87
F	-1.03	-1.01	-1.01	-1.01	-	-	-1.01	-1.01
CH_3-P	-1.27	-1.24	-1.26	-1.26	-1.21	-1.25	-	-
O-CH_3	-	-	-	-	-1.73	-1.72	-	-

Table 2

Simulated adsorption uptakes and enthalpies for sarin, soman, DMMP, DIFP and PMP in two representative MOF materials investigated in this study.

	Uptake $mmol.g^{-1}$					ΔH $kJ.mol^{-1}$				
	sarin	DMMP	DIFP	soman	PMP	sarin	DMMP	DIFP	soman	PMP
MIP-177-OH-H_2O	1.695	1.977	1.212	1.122	1.110	67.63	70.30	71.26	88.26	83.89
MOF-808-OH-H_2O	6.685	7.951	4.839	4.716	4.509	62.90	64.65	57.79	74.71	72.05

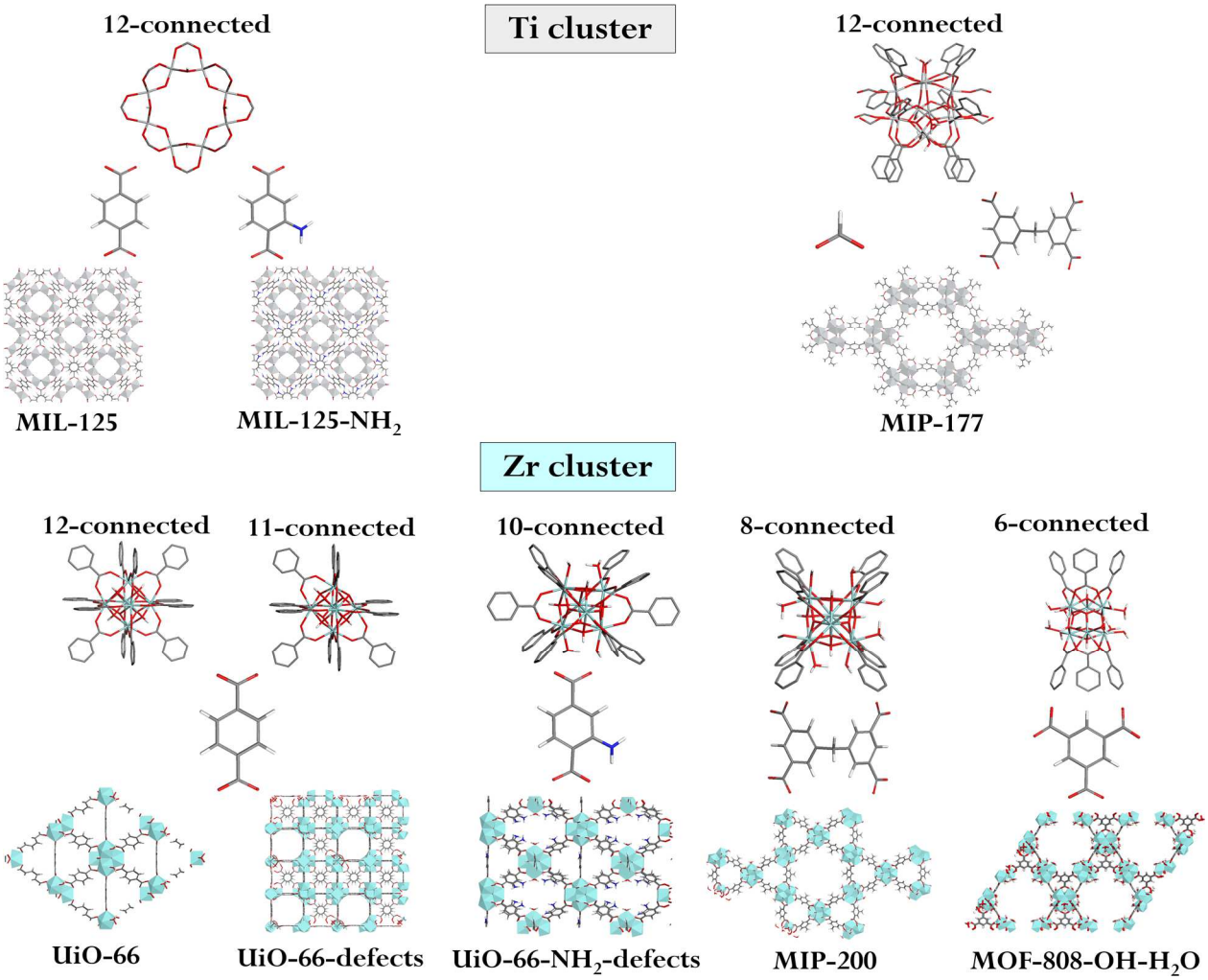

Fig. 1. Illustrations of the inorganic Zr and Ti building blocks present in a few representative 3D-MOFs considered in this work.

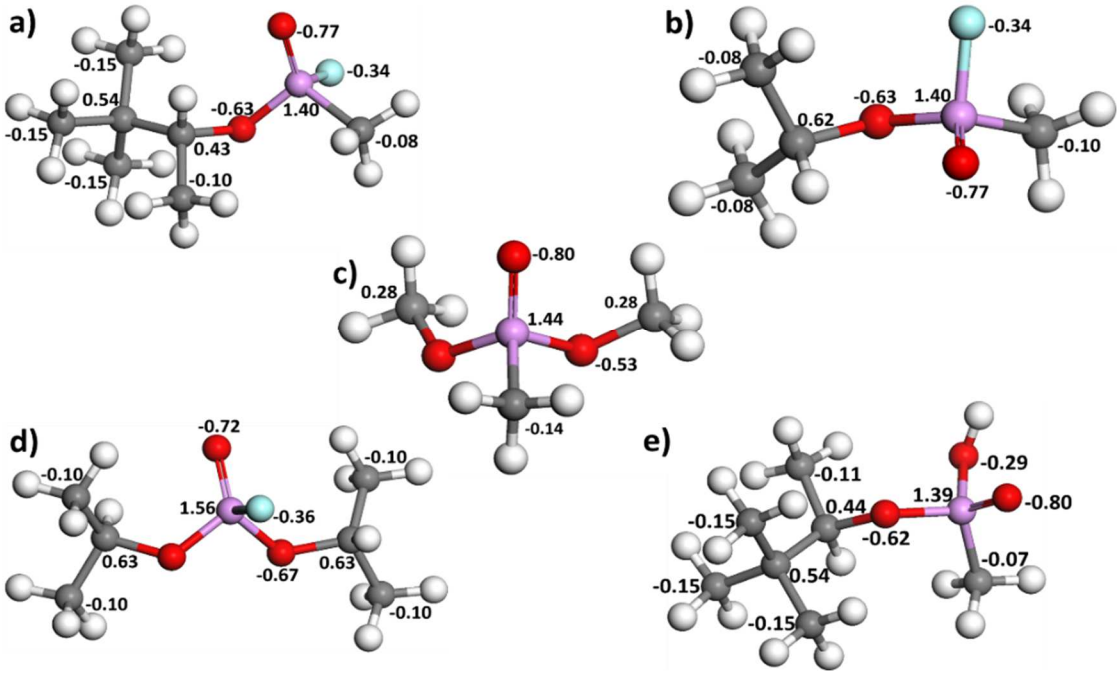

Fig. 2. Illustration of the CWAs molecules: (a) Soman, (b) Sarin, (c) DMMP, (d) DIFP and (e) PMP along with the partial charges used for the united-atom models considered in this work.

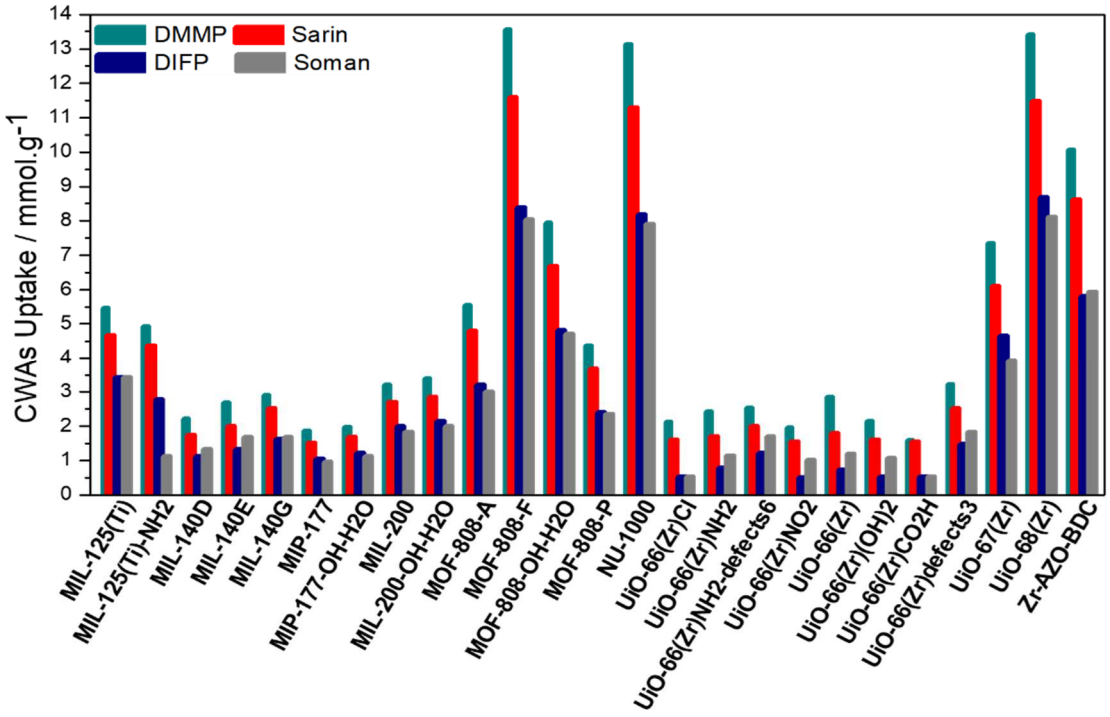

Fig. 3. GCMC simulated saturation uptakes at 298 K for all MOFs with respect to sarin, soman, DMMP and DIFP calculated using a pressure of 5000 kPa.

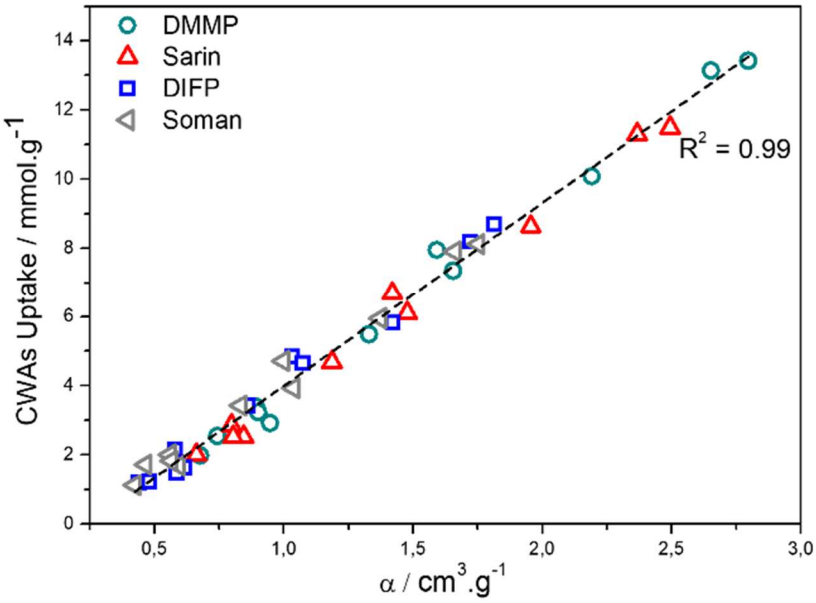

Fig. 4. Structure-adsorption uptake relationship for CWAs in MOFs.

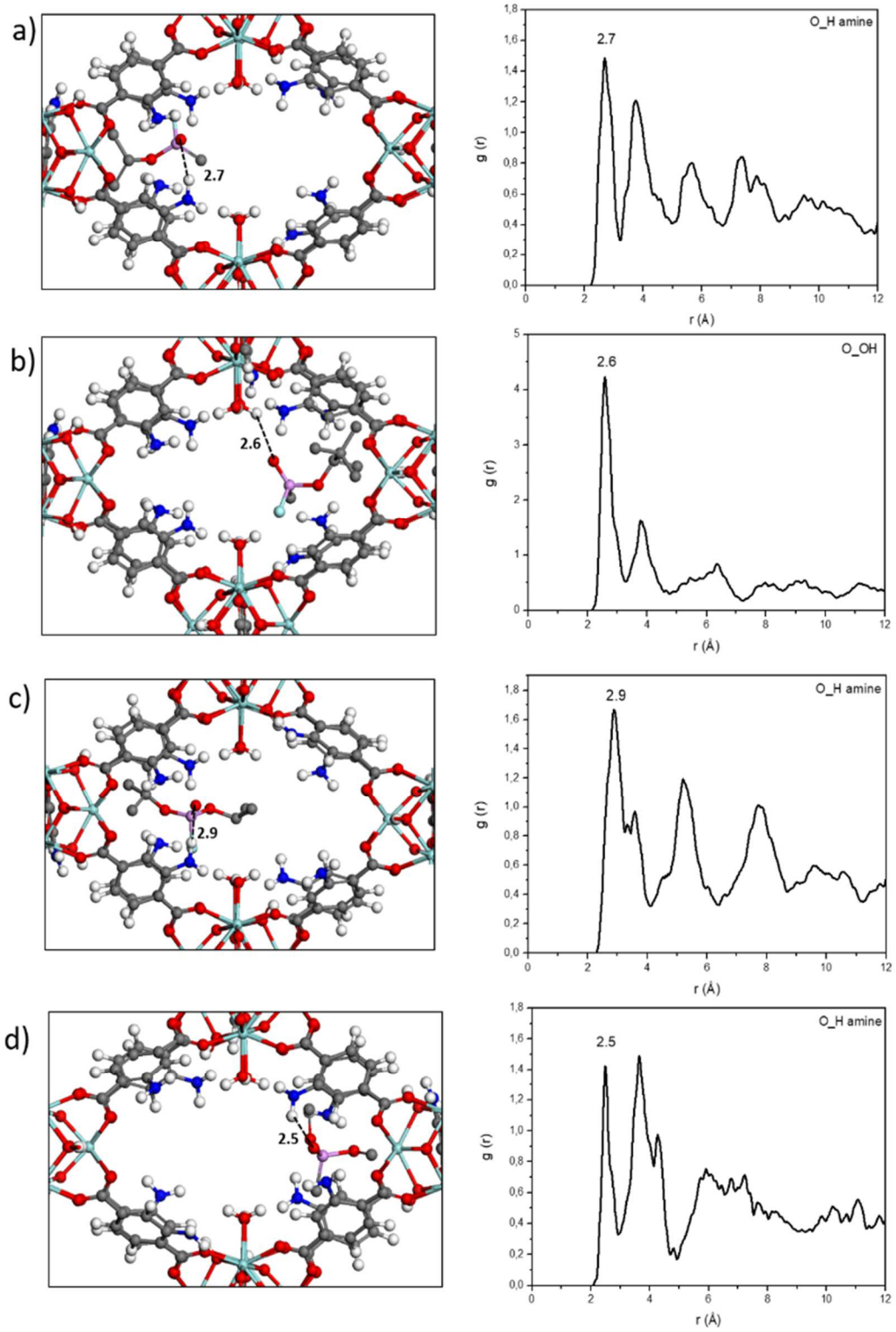

Fig. 5. A typical illustration of the preferential sittings for (a) Sarin, (b) Soman, (c) DIFP and (d) DMMP in the pores of the defective UiO-66(Zr)-NH_2 and the

corresponding CWA/MOF radial distribution functions averaged over all the MC configurations.

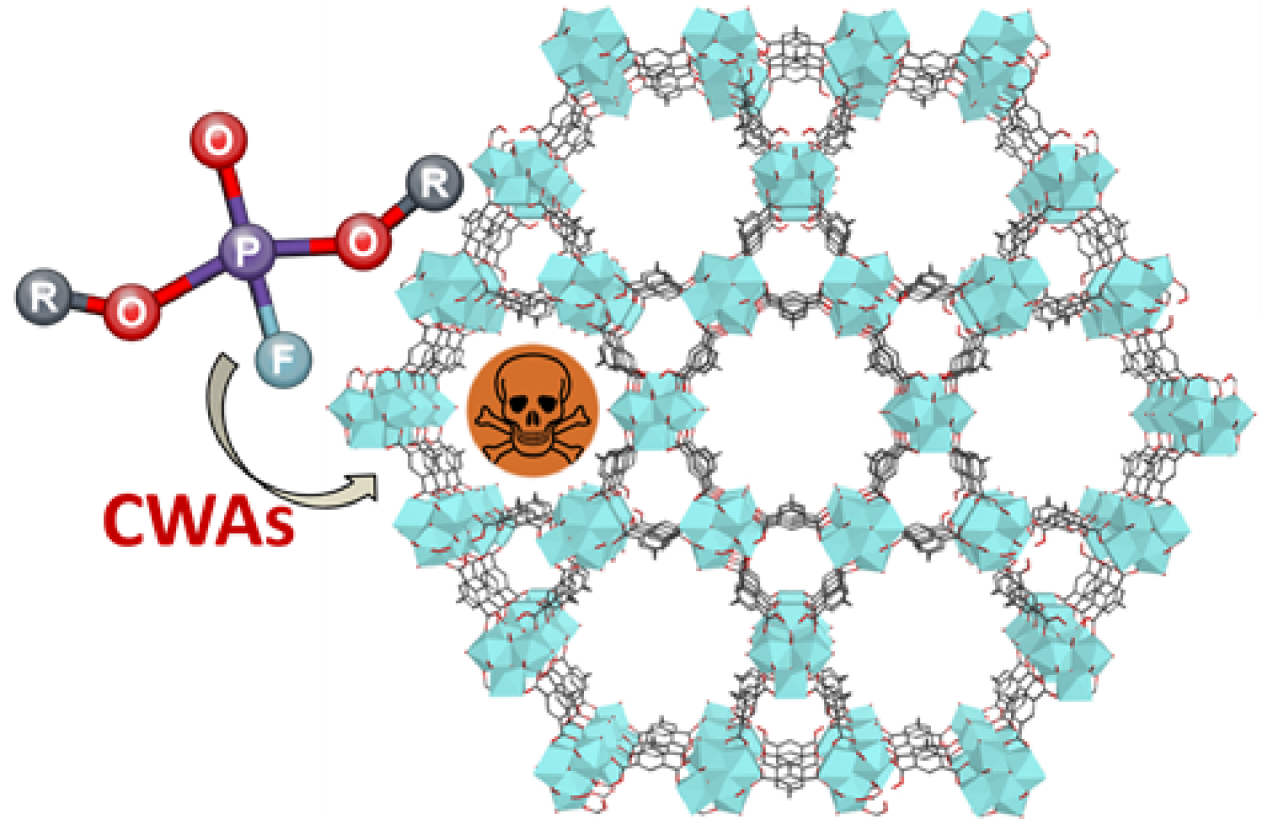
O
R
P
O
R
O
F
CWAs